Dynamic Channel Modeling for Underwater Magnetic Induction Communication

Wentao Zhou
School of Electronic Engineering
Soongsil University
Seoul, Korea
zwt@soongsil.ac.kr

Sai Wang
School of Electronic Engineering
Soongsil University
Seoul, Korea
wangsai@soongsil.ac.kr

Yoan Shin[§]
School of Electronic Engineering
Soongsil University
Seoul, Korea
yashin@ssu.ac.kr

***Abstract*—Nowadays, magnetic induction (MI) communication has been extensively studied mainly because it is less affected by environmental factors. Most research on MI communication assumes that the positions of the transmitter and the receiver are fixed and the channel hardly changes. The underwater environment characteristics are uncertain compared to the surface or the underground environments. When there is a water flow, the positions of the transmitter and the receiver change along with the communication channel. In this paper, we introduce the underwater omnidirectional MI structure and build a dynamic underwater MI model. Then, a path loss and a channel transfer function of this scenario are presented.**

***Index Terms*—Magnetic induction, underwater communication, omnidirectional structure, dynamic underwater environment, channel transfer function.**

I. Introduction

Acoustic communication is widely used in underwater environments. However, because of the Doppler effect, the salinity of seawater and the presence of electrical conductivity, the data rate is too low to achieve the purpose of high data rate communication. Optical communication has also been tried in underwater environments because of its high data rate capability, whereas it does not guarantee the stability of communication since it is hard to align the transmitter with the receiver. Electromagnetic communication is difficult to be used for long-distance underwater communication systems because of severe path loss triggered by water conductivity [1]. Hence, magnetic induction (MI) communication has been widely studied. Although the path loss of the MI communication system is still high, the energy is not consumed. Compared to the other three communication methods as mentioned earlier, MI communication is more effective and energy-efficient, which significantly improves the life cycle of wireless sensor networks.

Unlike the surface and the underground environments, the underwater environment is quite dynamic [2]. A large majority of researchers consider an ideal situation without water flow [3], which assumes a fixed transmitter and receiver. The MI structures are divided into two kinds: direct type MI and waveguide type MI. In the direct type MI structure, the transmitter communicates with the receiver directly, while the waveguide MI structure implies some relays between the transmitter and the receiver. These relays comprise coils that do not cost energy and just pass the energy from the previous coil to the next one [4]. In the early stages of MI research, research has focused on using unidirectional coils to find the relationship between the transmitter and the receiver. Because of the narrow bandwidth of the MI, the ways to improve the bandwidth have become an urgent problem. In [8], they use a multi-input multi-output (MIMO) configuration and the frequency splitting to achieve multiple modes. The crosstalk between transmitters can be canceled by the splitting frequency. The unidirectional MI MIMO structure has been well studied in [9]. The electric currents in the transmitters are opposite, then there is a cancellation plane between transmitters that can decrease the crosstalk of transceivers. Using the cancellation plane shows better performance than using the frequency splitting, but there is no contribution to improve the communication bandwidth. In [10], they use the same structure in [8], the resonant frequency of TX1 to RX1 and the resonant frequency of TX2 to RX2 are different. At the same time, they used metamaterial-enhanced MI to increase radiation efficiency. Although crosstalk still exists between the transceivers, the improvement in bandwidth allows MI communication to be better used in the future.

Researchers have found that the angles between the transmitter and the receiver antenna's coils can seriously affect the mutual inductance. The voltage of the receiver generated by the mutual inductance decreases as the mutual inductance decreases, and the path loss increases at the same time. This phenomenon is called polarization [5]. When the transmitter and the receiver's coils are parallel with each other and the center points are aligned, the mutual inductance reaches the maximum. Researchers also found that the omnidirectional MI structure shows a better performance than the unidirectional MI structure [6]. Therefore, from the transmitter and the receiver's antenna types, MI structures are divided into the unidirectional structure and the omnidirectional structure. The omnidirectional MI structures and experiments are introduced in [7]. The structure they used in this experiment is an omnidirectional MI with three switches, and the experimental environment is air. We can compute the channel transfer

[§] Corresponding author.

This work was supported by the NRF grant funded by the Korea government (MSIT) (2016R1A2B2014497).

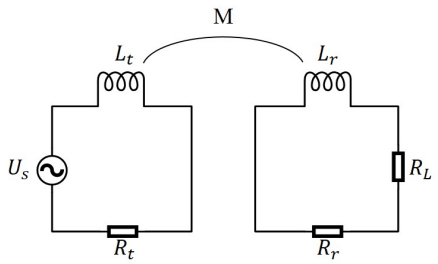

Fig. 1. Direct MI communication model.

function according to the model because the channel is stable. Under different operating modes and a few definite positions, they get the lifetimes and received voltages. In [11], they proposed a promising integration method for high-precision positioning and stable communication by using magnetic induction signals.

Most research on MI communication is still at the theoretical stage. In [12], they introduced the model of underwater MI communication, but they do not consider the path loss generated by the inverse of skin depth. The same issue occurs in [13]. Under the high operating frequency, the effective communication range is severely limited. Usually, we use the passive relay transceivers in the waveguide MI structure to improve the communication range. In [14], they use active relays to improve the performance of the receiver signal.

In this paper, we introduce an omnidirectional MI structure and construct a dynamic underwater channel model. Then, we compare the mutual inductance and the path loss of this structure with a unidirectional structure in our designed environment. Finally, we discuss the channel transfer function of our model. The remainder of this paper is structured as follows. Section II gives the background of the omnidirectional MI structure we used. Section III introduces the simulation scenario. Section IV shows the simulation and numerical results. And the channel transfer function is mentioned at the same time. Our conclusion is given in Section V.

II. System modeling

A. Polarization

The mutual inductance of two centers aligned and parallel coils can be calculated as [3]

$$M = \mu\pi N_t N_r \frac{a_t^2 a_r^2}{2r^2}, \tag{1}$$

where μ is the magnetic permeability (in the underwater environment, $\mu = 4\pi \times 10^{-7}$H/m). Also, N_t and N_r are the numbers of turns of the transmitter and the receiver antenna coils, respectively, a_t and a_r are the radius of the transmitter and the receiver antenna coils, respectively, and r is the distance between the transmitter and the receiver. As the distance increases, the mutual inductance decreases severely.

In the seawater environment, optical, electromagnetic, and magnetic field propagation speeds are approximately 3.33×10^7 m/s. Because the operating frequency of MI communication is quite low, the wavelength λ is much larger than communication distance d. This satisfies $\frac{\lambda}{2\pi} \gg d$, then the magnetic field within the radius R can be regarded as a quasi-static field [7]. In this condition, the magnetic field strength along the axis is much larger than other directions according to the right-hand screw rule, which demonstrates a strong directionality of the magnetic field. Based on this characteristic, the near-field MI communication parameters can be computed more precisely. On the other hand, because of the strong directionality, the polarization phenomenon exists between the transmitter and the receiver. In this structure, the mutual inductance can be calculated as [15]

$$M = \mu\pi N_t N_r \frac{a_t^2 a_r^2}{2r^2} \cdot J, \tag{2}$$

where J is the polarization factor. In 2-D space, J is defined as [16]

$$J_{2D} = \frac{1}{2}(2\sin\theta_t \sin\theta_r + \cos\theta_t \cos\theta_r), \tag{3}$$

where θ_t and θ_r are the angles between the magnetic field directions and the line connecting transmitter coils and receiver coils, respectively. In the 3-D space, we have to consider the situation where magnetic fields generated by transmitter coils and the receiver coils are not parallel. Let φ represent the angle between the above two magnetic field directions. We can easily get the polarization factor in 3-D space as [5]

$$J_{3D} = \frac{1}{2}(2\sin\theta_t \sin\theta_r + \cos\theta_t \cos\theta_r \cos\varphi). \tag{4}$$

B. MI Communication System Structure

Fig. 1 shows a typical direct-type MI communication structure. Both inductor L_t and resistance R_t are generated by the transmitter antenna coils, and inductor L_r and resistance R_r are generated by the receiver antenna coils. We can compute the resistance of the antenna coil [2]

$$R = \frac{N 2\pi a \rho}{A}, \tag{5}$$

where N is the number of turns, a is the radius, ρ is the electrical resistivity and A is the cross-sectional of wire. The self-induction L of the antenna coil is defined as [2]

$$L = \frac{\mu N^2 A}{l}, \tag{6}$$

where l is the length of the solenoid.

According to the Kirchhoff's law, the circuit equivalent formula is

$$Z_t I_t + j\omega M I_r = U_s, \tag{7}$$

$$(Z_r + Z_L) I_r + j\omega M I_t = 0, \tag{8}$$

where Z_t and Z_r are the impedances of the transmitter and the receiver without the load impedance, respectively. Also, I_t and I_r are the electric currents of the transmitter and the

receiver, respectively, Z_L is the load impedance in the receiver circuit, M is the mutual inductance, U_s is the power source, $\omega = 2\pi f$ is the angular frequency, and f is the operating frequency. Then we can get

$$I_r = -\frac{j\omega M I_t}{(Z_r + Z_L)}. \tag{9}$$

By solving (7) and (9), we also obtain

$$U_s = I_t[Z_t + \frac{\omega^2 M^2}{(Z_r + Z_L)}]. \tag{10}$$

The total resistance of the transmitter is

$$R_{t_{total}} = Z_t + \frac{\omega^2 M^2}{(Z_r + Z_L)}. \tag{11}$$

Z_t is defined as

$$Z_t = R_t + j\omega L_t. \tag{12}$$

The impedance Z_r without the load impedance Z_L is defined as

$$Z_r = R_r + j\omega L_r. \tag{13}$$

Normally, the varied load resistance will generate reflected power, which is considered as a loss in transmitter [17]. To reduce this phenomenon, it is better to set the load resistance to the conjugate of the receiver circuit impedance [3]. The load resistance is defined as

$$Z_L = \overline{Z_r + Z_r'}. \tag{14}$$

When adding a power source, i.e., $I_t = I_0 \cdot e^{-j\omega t}$, the transmitting power and the received power are defined as [3]

$$P_t = Re\{I_t^2 \cdot R_{t_{total}}\}, \tag{15}$$

$$P_r = Re\{I_r^2 \cdot Z_L\}. \tag{16}$$

The path loss is defined as

$$\begin{aligned} L_{MI(r)} &= 10\log_{10}\frac{P_t}{P_r} \\ &= Re\left\{-\frac{(Z_r + Z_L)\left(Z_t(Z_r + Z_L) + \omega^2 M^2\right)}{\omega^2 M^2 Z_L}\right\}. \end{aligned} \tag{17}$$

A magnetic field can be generated by an AC power source in the underwater environment. A negative influence exists at the same time that will change the distribution of the magnetic field because of the conductivity. As the operating frequency increases, this effect gets much stronger. This attenuation which is called the inverse of skin depth is defined as

$$\alpha = \frac{1}{\delta} = \sqrt{\pi f \mu \sigma}, \tag{18}$$

where σ is the electrical conductivity of water. Thus, the path loss generated by this phenomenon is [2]

$$PL_\alpha = 20\log_{10}(e^{\alpha r}). \tag{19}$$

As a result, the total path loss is

$$PL_{total} = PL + PL_\alpha. \tag{20}$$

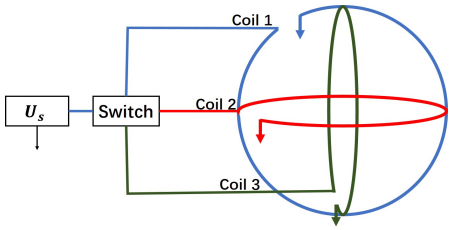

Fig. 2. Omnidirectional MI structure.

C. Channel and Noise

In deep water environments, there is no multipath interference in the MI communication channel because of the absence of reflection from the water surface and bottom sediments. Therefore, the MI communication channel is only affected by the path loss, which is determined by the mutual inductance of the transmitter and the receiver. Under different conditions (i.e., distance, coil deflection, transceiver's movement, etc.)the mutual inductances of transmitter coils and the receiver coils are different. Hence, the channel of MI communication is dynamic. As communication distance increases, the coupling of the two coils gets weaker. For the direct MI structure, the frequency splitting phenomenon does not occur because of the long transmission range.

In the MI communication structure, the main source of noise is the thermal noise generated by the resistance. The formula of this noise is expressed as

$$P_{dBm} = 10\log_{10}(k_B T f \times 1000), \tag{21}$$

where $k_B = 1.38 \times 10^{-23}\ J \cdot K^{-1}$ is the Boltzmann constant and T is the temperature of the communication environment.

Normally, we use

$$SNR = P_t - PL_{total} - P_{dBm} \tag{22}$$

to compute the signal-to-noise ratio. In (22), the total path loss can be computed according to some environment characteristics and the transceiver circuit parameters, and the power of thermal noise is also easy to compute. The remaining part is the power of the transmitter, and we can get the SNR after setting a proper value.

D. Omnidirectional MI Structure

The commonly used omnidirectional MI structures are shown in Fig. 2 [7]. In this structure, there are three strictly orthogonal coils. According to [19], there is no interference between these coils. In Fig. 2, three switches that can be freely controlled are added. In the process of communication, we can choose the largest mutual inductance between the transceivers by controlling the switches. In [7], they implement hardware with this structure. Regarding the structure, we can consider it as consisting of three unidirectional MI structures. By using equations given in II-B, we can calculate its path loss and channel transfer function.

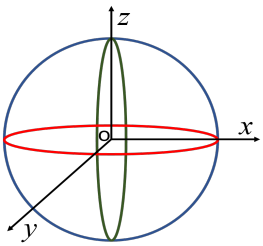

Fig. 3. Omnidirectional MI model with a Cartesian coordinate system.

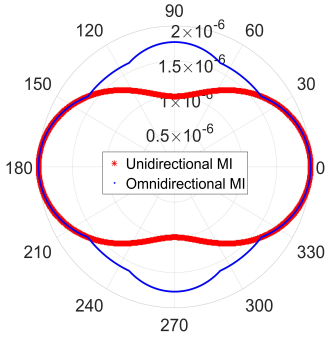

Fig. 4. Magnetic field strength on the XOY plane at a distance $r = 4$m.

E. Underwater Environments

Oceans cover about 70% of the earth's total area. A multitude of resources in the ocean is still undetected. Therefore, detecting underwater resources has become one of the most crucial processes of human development. The autonomous underwater vehicle (AUV) is a part of unmanned underwater vehicles that can complete most detection missions [20], e.g. water quality monitoring, underwater biological activity, searching plane wrecks, etc. The underwater environment is dynamic because of the random water flows. When an AUV is not affected by water flow, its buoyancy and gravity are equal. When an AUV is affected by water flow, the AUV can not at a fixed position, which severely affects the cooperation between the AUVs especially MI-based AUV. Quite a few kinds of AUV have the depth defining function and these AUVs can keep working at a specific depth. In actual use, an AUV is heavily affected by the water flow during the diving. When an AUV is at the bottom, the influence on the AUV reduces due to the small water flow, which hardly affects the operation of the equipment. In [20], an AUV named the UX-1 model is introduced. The results manifest that the movement of UN-1 does not strictly follow the planned path. Water flows with different strengths act on the AUV, and AUV displacement and angular deflection are different. The force analysis of AUV in the underwater environment is described in [21].

The speed of water flow in the deep sea environment has been introduced in [22]. An example was given about water flow speed under the different depth of Gulf Stream. As depth close to -2000 m, the water flow velocity approaches 0. When the depth exceeds -2000m, the reverse speed gradually increases. Hence, the AUVs in the underwater environment move randomly because of the water flow's different directions. The maximum speed for the Gulf Stream is 2.5m/s, and the speeds for deep currents vary from 0.02 to 0.1m/s or less.

III. Mutual Inductance at Different Positions

In this section, we introduce how to compute the mutual inductance and the path loss between two moving transceivers.

Because the antenna coils are strictly orthogonal with each other, we set a model with a Cartesian coordinate system shown in Fig. 3. We name the coil parallel to the XOY plane as C_{xoy}, and the coil parallels to the YOZ plane as C_{yoz}, the coil parallel to the ZOX plane as C_{zox}. We observe that the direction of the magnetic field generated by any coil is parallel to the coordinate axis which is not coplanar with it. Hence, we choose the axis to present its magnetic field direction, i.e., the direction of the magnetic field generated by C_{xoy} is a vector in the z-axis direction. We assume that the transmitter and the receiver are in a large Cartesian coordinate system and can be moved and flipped. A typical example should be cited that transmitter coordinate is (x, y, z) without flipping, then we can consider the magnetic field of C_{xoy} is $(x, y, 1)$, the magnetic field of C_{yoz} is $(1, y, z)$, and the magnetic field of C_{zox} is $(x, y, 1)$.

In the Cartesian coordinate system, we can use v=$x\hat{i}$+$y\hat{j}$+$z\hat{k}$ represent a vector. If there are two vectors v_1 and v_2, we can use

$$\alpha = \cos^{-1}\left(\frac{v_1 \cdot v_2}{|v_1| \cdot |v_2|}\right) \tag{23}$$

to find the angle between them. In the omnidirectional MI structure, we can figure out the angles between transceivers and the connection between them, i.e., θ_t and θ_r. We can also calculate the angle between every transmitter coil and every receiver coil θ_φ. According to (5), we can calculate the polarization factor. Then we choose the maximum polarization factor to compute the mutual inductance M and the path loss.

IV. Simulation and Numerical Results

A. MI Structures

In this section, we introduce our simulation model and numerical results. The transceiver antenna coil parameters are as follows: the cross-sectional area A for copper wire is 1.65 mm^2, the electrical resistivity of copper ρ is 0.01724 ohm $\cdot$ mm^2/m, the solenoid length l is 6m. The coil radius a and the number of turns of C_{xoy} are 0.45m and 50, respectively. Then, the coil radius a and the number of turns of C_{yoz} are 0.5m and 40, respectively. Lastly, the coil radius a and the number of turns of C_{zox} are 0.55m and 35, respectively. The simulation environment is deep seawater where conductivity σ is 4 S/m, the speed of water flow is 0.2m/s and the temperature is 276.15 K. The operating frequency is 3000Hz.

Fig. 4 shows mutual inductance evaluated on the XOY plane at a distance $r = 4$m. In these two curves, we set the flip angle 0. As we can see, the omnidirectional MI structure has a better performance on the mutual inductance. The mutual

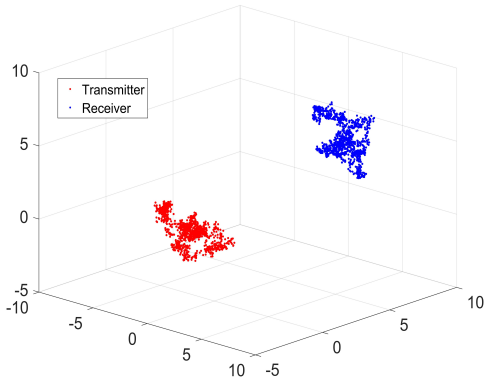

Fig. 5. Trajectories of the transceivers.

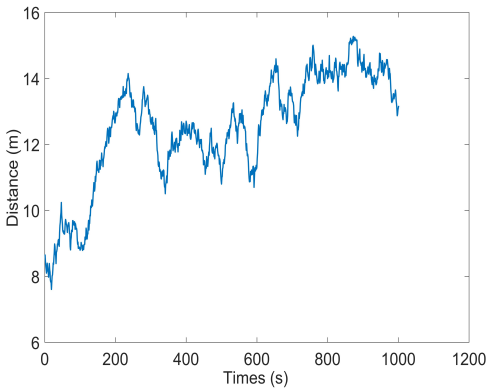

Fig. 6. Distance between transceivers.

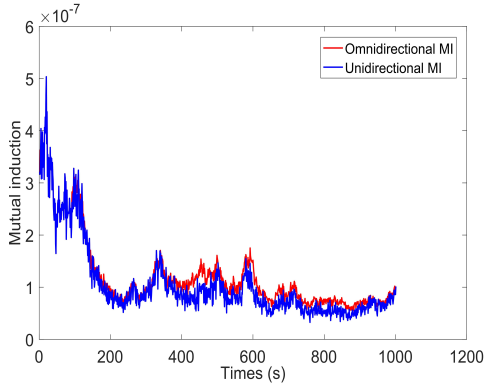

Fig. 7. Mutual inductance over time.

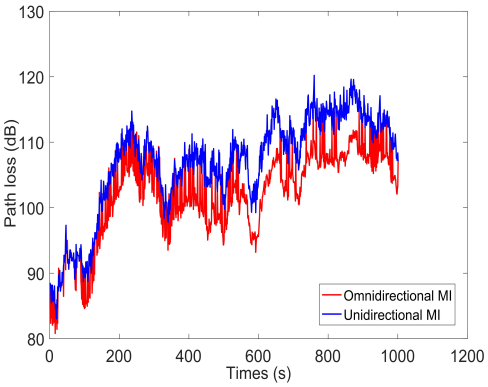

Fig. 8. Total path loss over time.

inductance is concave at 38° and 65.6°, the other quadrants are symmetrical. That is because a choice process occurs at the transceivers in these angles.

We simulate the model with a dynamic underwater environment. Fig. 5 shows the trajectories of the transceivers which affected by the water flow. We assume that transceiver speed is 0.02 m/s with random direction. The transceivers can move against the water flow, the total shift of transceivers is 0. At the same time, there is an angle deflection in every transceiver. Fig. 6 shows the distance between the transmitter and the receiver. The total distance varies because of transceiver movements. Fig. 7 shows the changes in the mutual inductance in the omnidirectional MI structure and the unidirectional MI structure over time. In the beginning, their performances are much similar. However, when the position and the angle change as time increases, the omnidirectional MI structure is much better than the unidirectional structure, while the difference between them is not too much. The total path losses are shown in Fig. 8. The unidirectional MI's path loss is much larger than the omnidirectional MI. The mutual inductance and the path loss vary with distance and angle deflection. Thus, in the dynamic underwater environment, the omnidirectional MI structure can increase performance effectively.

B. Channel Estimation

In this section, the dynamic underwater channel is discussed. In [15], they discuss that orthogonal frequency division multiplexing (OFDM) modulation is hard to be used in MI communication. To decouple the OFDM blocks and to enable the cyclic convolution in the OFDM, the cyclic prefix (CP) has to be added. The length of CP is at least as long as the channel impulse response, which lasts over 10000 taps. This phenomenon decreases the date rate. Typically, the output $y(n)$ of the OFDM system is the convolution of the input $x(n)$ and the channel transfer function $h(n)$. When there are m paths in this model, the output is

$$y(n) = h_1(n) * x(n) + \cdots + h_m(n) * x(n - l_m), \qquad (24)$$

where $h_m(n)$ is the channel impulse response of the m-th path, "$*$" represents the convolution and the $x(n - l_m)$ represents the data after the cyclic shift of the transmitted data corresponding to the m-th path. After the discrete Fourier transform (DFT), the frequency domain is

$$Y(k) = H_1(k)X(k) + \cdots + H_m(k)X(k) \cdot e^{jwl_m}. \qquad (25)$$

The sub-carriers are still orthogonal in the frequency domain after the cyclic shift. This process does not cause inter-symbol interference (ISI) so that every sub-carrier only multiplies an

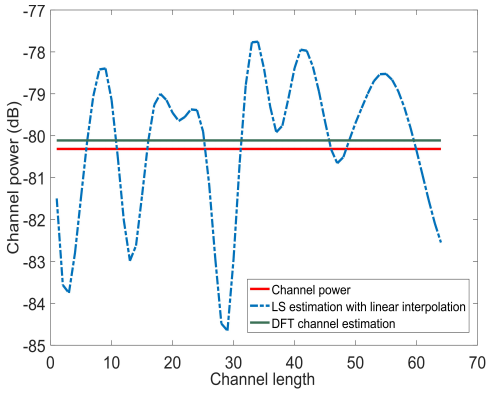

Fig. 9. Underwater MI channel estimation based on LS and DFT.

angle shift. We can use the equalizer to estimate the original channel.

In the omnidirectional MI structure, the transceivers can choose the largest mutual inductance mode that means the path loss and the channel changed by time, which means it is a time-varying channel. There is no reflected magnetic field in the deep-water environment, which means there is no multipath fading in the underwater MI channel. In this case, the output is

$$Y(k) = H(k)X(k). \tag{26}$$

Generally, the transmission distance is a few meters, so the delay is within 1 μs. When OFDM is the modulation scheme, the delay is much smaller than the length of the CP. We can choose a short CP because of the single transmission path, and the resulting impulse response is extremely short. We do not have to set a long filter for channel estimation. Although the underwater MI channel is dynamic, the channel transfer function is stable in every state. We can use OFDM as the modulation scheme and use an equalizer to estimate the channel.

We choose positions (0,0,0) and (5,5,5) for the transmitter and the receiver, respectively. In this scenario, the channel transfer function is $\sqrt{\frac{10^{(-PL/10)}}{2}}(randn + jrandn)$. We use OFDM modulation with 64 sub-carriers and 8 pilots for channel estimation. So, the channel length is 64. Fig. 9 shows an example MI channel function estimated by the least square (LS) channel estimator with linear interpolation, and the channel is estimated again by a DFT estimator after the LS channel estimator. According to Fig. 9, we observe that the MI channel is easy to estimate because there is no multipath fading in the underwater environment.

V. Conclusion

In this paper, we introduced an underwater MI omnidirectional structure and a dynamic underwater environment and compared the performances of the omnidirectional MI structure with the unidirectional MI structure. Finally, we introduced the channel of underwater MI and proved that OFDM modulation could be effectively used in our communication system.

References

[1] M. Mostafa, H. Esmaiel, and E. M. Mohamed, "A comparative study on underwater communications for enabling C/U plane splitting based hybrid UWSNs," *Proc. IEEE WCNC2018*, Barcelona, Spain, Apr. 2018.

[2] M. C. Domingo, "Magnetic induction for underwater wireless communication networks," *IEEE Trans. Antennas & Propag.*, vol. 60, no. 6, pp. 2929-3939, Apr. 2012.

[3] Z. Sun and I. F. Akyildiz, "Magnetic induction communications for wireless underground sensor networks," *IEEE Trans. Antennas & Propag.*, vol. 58, pp. 2426-2435, July 2010.

[4] Z. Sun and I. F. Akyildiz. "Underground wireless communication using magnetic induction," *Proc. IEEE ICC2009*, Dresden, Germany, June 2009.

[5] S. Kisseleff, I. F. Akyildiz, and W. Gerstacker, "Interference polarization in magnetic induction based wireless underground sensor networks," *Proc. IEEE PIMRC2013*, London, UK, Sept. 2013.

[6] I. F. Akyildiz, P. Wang, and Z. Sun, "Realizing underwater communication through magnetic induction," *IEEE Commun. Mag.*, vol. 53, no. 11, pp. 42-48, Nov. 2015.

[7] N. Ahmed, A. Radchenko, D. Pommerenke, and Y. R. Zheng, "Design and evaluation of low-cost and energy-efficient magneto-inductive sensor nodes for wireless sensor networks," *IEEE Systems Jour.*, pp. 1-10, Aug. 2018.

[8] H. Nguyen, J. I. Agbinya, and J. Devlin, "FPGA-based implementation of multiple modes in near field inductive communication using frequency splitting and MIMO configuration," *IEEE Trans. Circuits & Syst.*, vol. 62, no. 1, pp. 302-310, Jan. 2015.

[9] H. Kim, J. Park, K. Oh, J. Choi, J. E. Jang, and J. Choi, "Near-field magnetic induction MIMO communication using heterogeneous multipole loop antenna array for higher data rate transmission," *IEEE Trans. Antennas & Propag.*, vol. 64, no. 5, pp. 1952-1962, Mar. 2016.

[10] H. Guo and Z. Sun, "Increasing the capacity of magnetic induction communication using MIMO coil-array," *Proc. IEEE GLOBECOM2016*, Washington DC, USA, Dec. 2016.

[11] H. Wu, X. Jiang, P. Xu, and C. Zhang, "Efficient integration of magnetic positioning and stable communications," *IEEE Magnetics Lett.*, vol. 9, pp. 1304404, July 2018.

[12] B. Gulbahar and O. B. Akan, "A communication theoretical modeling and analysis of underwater magneto-inductive wireless channels," *IEEE Trans. Wireless Commun.*, vol. 11, no. 9, pp. 3326-3334, Sept. 2012.

[13] J. Zhou and J. Chen, "Maximum distance estimation of far-field model for underwater magnetic field communication," *Proc. IEEE CCWC2017*, Las Vegas, NV, USA, Mar. 2017.

[14] S. Kisseleff, B. Sackenreuter, I. F. Akyildiz, and W. Gerstacker, "On capacity of active relaying in magnetic induction based wireless underground sensor networks," *Proc. IEEE ICC2015*, London, UK, Sept. 2015.

[15] S. Kisseleff, I. F. Akyildiz, and W. H. Gerstacker, "Digital signal transmission in magnetic induction based wireless underground sensor networks," *IEEE Trans. Commun.*, vol. 63, no. 6, pp. 2300-2311, June 2015.

[16] Z. Sun and I. F. Akyildiz, "On capacity of magnetic induction-based wireless underground sensor networks," *Proc. IEEE INFOCOM2012*, Orlando, USA, Mar. 2012.

[17] K. Sugeno, S. Noguchi, M. Inamori, and Y. Sanada, "Effect of load fluctuation in data transmission for wireless power transfer," *Proc. IEEE PIMRC2012*, Sydney, Australia, Sept. 2012.

[18] J. I. Agbinya, "A magneto-inductive link budget for wireless power transfer and inductive communication systems," *Progress in Electromag. Research C*, vol. 37, pp. 15-28, 2013.

[19] N. Ahmed, Y. R, Zheng, and D. Pommerenke, "Theoretical modeling of multi-coil channels in near field magneto-inductive communication," *Proc. IEEE VTC2015*, Boston, USA, Sept. 2015.

[20] R. A. S. Fernandez, D. Grande, A. Martins, L. Bascetta, S. Dominguez, and C. Rossi, "Modeling and control of underwater mine explorer robot UX-1," *IEEE Access*, vol. 7, pp. 39432-39447, Mar. 2019.

[21] T. I. Fossen, *Handbook of Marine Craft Hydrodynamics and Motion Control*, Ch. 8, Wiley, 2011.

[22] R. H. Stewart, *Introduction to Physical Oceanography*, Ch. 10, Prentice Hall, 2008.